

Modified kinetic theory applied to the shear flows of granular materials

Yifei Duan, Zhi-Gang Feng, Efstathios E. Michaelides, and Shaolin Mao

Citation: *Physics of Fluids* **29**, 043302 (2017); doi: 10.1063/1.4979632

View online: <http://dx.doi.org/10.1063/1.4979632>

View Table of Contents: <http://aip.scitation.org/toc/phf/29/4>

Published by the [American Institute of Physics](#)

Articles you may be interested in

[Preface to Special Topic: A Tribute to John Lumley](#)

Physics of Fluids **29**, 020501020501 (2017); 10.1063/1.4976616

[On the shape memory of red blood cells](#)

Physics of Fluids **29**, 041901041901 (2017); 10.1063/1.4979271

[Exact analytical solution for large-amplitude oscillatory shear flow from Oldroyd 8-constant framework: Shear stress](#)

Physics of Fluids **29**, 043101043101 (2017); 10.1063/1.4978959

[Editorial: In defense of science—What would John do?](#)

Physics of Fluids **29**, 020602020602 (2017); 10.1063/1.4974531

[Simulation of liquid jet atomization coupled with forced perturbation](#)

Physics of Fluids **29**, 022103022103 (2017); 10.1063/1.4976621

[Particle resolved simulations of liquid/solid and gas/solid fluidized beds](#)

Physics of Fluids **29**, 033302033302 (2017); 10.1063/1.4979137

Fearful for the future of science?

Sign up for **FREE** FYI emails.
AIP | American Institute of Physics

Modified kinetic theory applied to the shear flows of granular materials

Yifei Duan,¹ Zhi-Gang Feng,^{1,a)} Efstathios E. Michaelides,² and Shaolin Mao³

¹Department of Mechanical Engineering, UTSA, San Antonio, Texas 78249, USA

²Department of Engineering, TCU, Fort Worth, Texas 76129, USA

³Department of Mechanical Engineering, UTEP, El Paso, Texas 79902, USA

(Received 5 October 2016; accepted 21 March 2017; published online 11 April 2017)

Granular materials are characterized by large collections of discrete particles, where the particle-particle interactions are significantly more important than the particle-fluid interactions. The current kinetic theory captures fairly accurately the granular flow behavior in the dilute case, when only binary interactions are significant, but is not accurate at all in the dense flow regime, where multi-particle interactions and contacts must be modeled. To improve the kinetic theory results for granular flows in the dense flow regime, we propose a Modified Kinetic Theory (MKT) model that utilizes the contact duration or cutoff time to account for the complex particle-particle interactions in the dense regime. The contact duration model, also called TC model, was originally proposed by Luding and McNamara [“How to handle the inelastic collapse of a dissipative hard-sphere gas with the TC model,” *Granular Matter* **1**, 113 (1998)] to solve the inelastic collapse issue existing in the inelastic hard sphere model. This model defines a cutoff time t_c such that dissipation is not counted if the time between two consecutive contacts is less than t_c . As shown in their study, the use of a cutoff time t_c can also reduce the dissipation during multi-particle contacts. In this paper we relate the TC model with the Discrete Element Method (DEM) by choosing the cutoff time t_c to be the duration of contact calculated from the linear-spring-dashpot soft-sphere model of the DEM. We examine two types of granular flows, simple shear flow and the plane shear flow, and compare the results of the classical kinetic theory model, the present MKT model, and the DEM model. We show that the MKT model entails a significant improvement over the kinetic theory model for simple shear flows at inertial regimes. With the MKT model the calculations are close to the DEM results at solid fractions as high as 0.57. Even for the plane shear flows, where shear rate and solid fraction are inhomogeneous, the results of the MKT model agree very well with the DEM results. *Published by AIP Publishing.* [<http://dx.doi.org/10.1063/1.4979632>]

I. INTRODUCTION

The study of granular flow is of interest in a wide variety of fields in fundamental and applied science, including industrial flows (pneumatic conveying and fluidized bed reactors) and environmental flows (sand dunes and snow avalanches). Granular matter under rapid flow conditions is most commonly modeled as a continuum phase. The kinetic theory, supplemented with numerical simulations, is considered to be one of the best tools to describe the behavior of granular flows. Various forms of the classical kinetic theory have been derived for a system under the assumption that only instant binary collisions occur.²⁻⁴ This assumption is satisfied in relatively dilute regimes, where the volume fraction of solid particles varies between 0 and 0.49.⁵ The classical kinetic theory models exhibit a general good agreement with numerical simulations following the discrete element method (DEM).⁶⁻⁸ However, in the dense regime, where sustained multi-particle contacts are significant, the simulation results based on the classical kinetic theory model are not accurate, especially at very high solid fractions.^{5,9}

Most of the granular flows with practical interest are dense flows. Two approaches have been proposed to model granular flows in the dense regime: The first is entirely phenomenological and makes use of dimensional analysis to identify the dimensionless parameters that govern the problem. The solution of this approach includes algebraic relations between those parameters (i.e., the granular local rheology).¹⁰⁻¹³ However, this approach is not systematic and is limited to very dense and steady cases, such as chute flows. The second approach is more fundamental and is based on the kinetic theory. Part of this approach is to include a frictional force, borrowed from soil mechanics, to the constitutive relations of the classical kinetic theory. The frictional force takes into account the effects of particulate contacts near the maximum packing density of the material.^{14,15} Studies have shown that granular flow involves a reduced collisional dissipation rate and an increased collision frequency in the dense regime.¹⁶⁻¹⁸ The simplest way to account for this effect is to modify the radial distribution function and energy dissipation term in the energy conservation equation.

Among the modifications to the energy dissipation rate, one is the Extended Kinetic Theory (EKT) proposed by Jenkins and co-workers,¹⁹⁻²¹ which involves the incorporation of a length-scale other than the particle diameter in the

^{a)}Electronic mail: zhigang.feng@utsa.edu

expression for the rate of collisional dissipation. This revised model includes a material coefficient of unclear meaning, which is considered to be a weakness of the theory by a few researchers.¹³ Other modifications for denser systems such as those by Chialvo and Sundaresan^{5,9} which are based on the DEM simulations of homogeneous simple shear flow include the following: (a) an effective restitution coefficient to capture the increased granular energy dissipation rate due to friction;²² (b) a new expression for the radial distribution function at contact;²³ and (c) a chain length to account for the reduced granular energy dissipation rate.²¹ As a result of the modifications, the theoretical predictions of the models based on the kinetic theory show good agreement with the numerical data of the DEM simulations. Most of the modifications to the kinetic theory models apply or have been only verified for steady uniform shear flows and homogeneous cooling processes. Because of the nature of practical systems such as fluidized beds, one expects that the granular temperature, the shear rate, and the solid volume fraction are unsteady nonhomogeneous parameters that vary across the flow domain. In addition, some constitutive laws such as the proportional relation between the shear stress and the square of the strain-rate (i.e., the Bagnold's scaling)²⁴ are not applicable in flows with a non-uniform shear rate.²⁵ Therefore, the modifications of the kinetic theory based on simple shear flow simulations may not be suitable for non-uniform flows; a more general modification of kinetic theory will be needed for these cases.

Similar to the kinetic theory model, the Inelastic Hard Sphere (IHS) also assumes that the collisions are instantaneous and uncorrelated. For this reason, the results of IHS simulations and kinetic theory solutions typically agree very well. However, the kinetic theory and the IHS start to deteriorate as the solid fraction of a granular flow increases because of the overestimate of energy dissipation during particle collisions. Luding and McNamara¹ addressed this problem by introducing a contact duration. A particle has the memory of its last contact, so a new contact occurring within t_c (the contact duration) after the last contact is a multi-particle contact and has no further energy dissipation (TC model).^{1,26} t_c is a number that modifies the amount of dissipation due to collisions. However, the question of how to choose the proper value of t_c for a specific granular flow system has not been studied.

The DEM model mimics a real system where the particle collision is a process that takes finite time to complete. Therefore, in the DEM model the kinetic energy may be converted into the elastic potential energy during the contact. This elastic, potential energy is not dissipated. The main contribution of this paper is to use the DEM model to determine the amount of elastic energy that needs to be detained in the modified kinetic theory (MKT). Since the elastic potential energy in the DEM is related to the spring constant which determines the collision contact time t_{DEM} and the cutoff time t_C in the extended IHS is used to modify the energy dissipation, we propose the use of t_{DEM} as the cutoff time t_C in the MKT. This allows us to calculate the elastic potential energy in the MKT model that exists in the dense region. We further extend the MKT to examine simple shear flows and plane shear flows at a high solid volume fraction, compare the results of the classical kinetic theory model, the present MKT model, and the DEM model,

and evaluate its applicability and limitations. The aim of this paper is to provide such a general modification to the kinetic theory when it is applied to the dense flow regions. This paper also addresses the observed higher estimate of energy dissipation rate of granular inhomogeneous flows at high solid volume fractions when the binary collision assumption of the kinetic theory is no longer valid. Overall the MKT model is a significant improvement over the classical kinetic theory model for all the cases we have studied. It is capable to produce results that are close to the DEM results at solid fractions as high as 0.57, when the flow is still in the inertial region. Even for plane shear flows, where the shear rate and the solid fraction are non-homogeneous, the MKT results agree very well with the DEM results

II. THE KINETIC THEORY OF GRANULAR FLOW

In modeling particulate or granular flows, the kinetic theory is commonly used to obtain the constitutive relations for the particulate phase. The most commonly used kinetic theory models have been derived for dilute flows of smooth, frictionless spheres and are basically extensions of the classical kinetic theory of non-uniform gases.^{2,27,28} One important difference between particles and gas molecules is that the kinetic energy is conserved in the elastic molecule collisions, but not in inter-particle collisions because these collisions are inelastic. In the context of kinetic theory, a single-particle distribution function $f(\mathbf{v}, \mathbf{x}, t)$ governs the macroscopic properties of solid particles. Hence, the hydrodynamic governing equations of motion are obtained by the appropriate transformations of the time evolution equation for $f(\mathbf{v}, \mathbf{x}, t)$. The distribution function for the positions and velocities of smooth spheres is described as follows:

$$\frac{\partial f}{\partial t} + \mathbf{v} \cdot \nabla f = J[f, f], \quad (1)$$

$$J[f, f] = d^2 \int d\mathbf{v}_2 \int \Theta(\mathbf{g} \cdot \mathbf{n})(\mathbf{g} \cdot \mathbf{n}) \times \left[\frac{1}{e^2} f_2(\mathbf{v}'_1, \mathbf{x}_1, \mathbf{v}'_2, \mathbf{x}_1 - d\mathbf{n}, t) - f_2(\mathbf{v}_1, \mathbf{x}_1, \mathbf{v}_2, \mathbf{x}_1 + d\mathbf{n}, t) \right] d\mathbf{n}, \quad (2)$$

where e is the particle restitution coefficient, d is the particle diameter, f_2 is the pair-distribution function, and $J[f, f]$ is the collisional term. At time t , velocities \mathbf{v}_1 and \mathbf{v}_2 of two particles are, respectively, changed to \mathbf{v}'_1 and \mathbf{v}'_2 by the collision. The relative velocities $\mathbf{g} = \mathbf{v}_1 - \mathbf{v}_2$ and \mathbf{n} is the unit vector from the center of particle 1 to that of particle 2. The Heaviside step function Θ assures that the relative velocities \mathbf{g} are such that a collision takes place. From these expressions, we may obtain the balance equations for mass, momentum, and energy by multiplying m , $m\mathbf{v}$, and $m\mathbf{v}^2/2$ to the kinetic equation and integrate over the velocity space \mathbf{v} , as shown in the following equations:²⁹

$$\frac{\partial \rho}{\partial t} + \rho \nabla \cdot \mathbf{u} = 0, \quad (3)$$

$$\rho \frac{D\mathbf{u}}{Dt} + \nabla \cdot \boldsymbol{\sigma} = 0, \quad (4)$$

TABLE I. Summary of the model equation.⁴⁹

$$p^* = 1 + 2(1 + e)\phi g_0$$

$$p = \rho\phi T p^*$$

$$\Gamma = \frac{12}{\sqrt{\pi d}} \rho \phi^2 g_0 (1 - e^2) T^{\frac{3}{2}} K$$

$$\tau = -2\eta S - \gamma \delta_{ij} \nabla \cdot \mathbf{u}$$

$$c^* = \frac{32(1-e)(1-2e^2)}{81-17e+30e^2(1-e)}$$

$$\zeta^{0*} = \frac{5}{12} g_0 (1 - e^2) (1 + \frac{3}{32} c^*)$$

$$\gamma^* = \frac{128}{5\pi} \phi^2 g_0 (1 + e) (1 - \frac{c^*}{32})$$

$$\eta_k^* = \left[1 - \frac{2}{5} (1 + e) (1 - 3e) \phi g_0 \right] / (v \eta^* - \frac{1}{2} \zeta^{0*})$$

$$\eta^* = \eta_k^* \left[1 + \frac{4}{5} \phi g_0 (1 + e) \right] + \frac{3}{5} \gamma^*$$

$$\eta_0 = \frac{5}{16d^2} \left(\frac{mT}{\pi} \right)^{\frac{1}{2}}, \eta = \eta_0 \eta^*, \gamma = \gamma^* \eta_0$$

$$q = -\kappa \nabla T - \mu \nabla \phi$$

$$v_k^* = \frac{1}{3} (1 + e) g_0 \left[1 + \frac{33}{16} (1 - e) + \frac{19-3e}{1024} c^* \right]$$

$$\kappa^{k*} = \frac{2}{3} \left\{ 1 + \frac{1}{2} (1 + p^*) c^* + \frac{3}{5} \phi (1 + e)^2 \left[2e - 1 + \left(\frac{1}{2} (1 + e) - \frac{5}{3(1+e)} \right) c^* \right] \right\} / (v_k^* - 2\zeta^{0*})$$

$$\kappa_0 = \frac{15}{4} \eta_0, \kappa = \kappa_0 \kappa^*$$

$$\mu^{k*} = \left\{ \left(1 + \phi \frac{dg_0}{d\phi} \right) \zeta^{0*} \kappa^{k*} + \left(\frac{v_k^*}{3} + \frac{2}{3} \phi (1 + e) \left(g_0 + \phi \frac{dg_0}{d\phi} \right) \right) c^* - \frac{4}{5} \phi g_0 \left(1 + \frac{\phi}{2} \frac{dg_0}{d\phi} \right) (1 + e) (e(1 - e) + \frac{1}{4} \left(\frac{4}{3} + e(1 - e) \right) c^*) \right\} / (2v_k^* - 3\zeta^{0*})$$

$$\mu^* = \mu^{k*} \left[1 + \frac{6}{5} \phi g_0 (1 + e) \right]$$

$$\mu = \pi d^3 T \kappa_0 / 6\phi$$

$$\frac{3}{2} \rho \frac{DT}{dt} + \nabla \cdot \mathbf{q} + \boldsymbol{\sigma} : \boldsymbol{\varepsilon} + \Gamma = 0. \quad (5)$$

In the last set of equations $\mathbf{u} = \langle \mathbf{v} \rangle = \frac{1}{n} \int f(\mathbf{v}, \mathbf{x}, t) \mathbf{v} d\mathbf{v}$ is the mean velocity of the flow; $V = |\mathbf{v} - \mathbf{u}|$ is the magnitude of the particles' fluctuating velocity; ρ , $\boldsymbol{\sigma}$, $\boldsymbol{\varepsilon}$ are the density, the stress, and strain rate tensor of solid phase, respectively, and $T = \frac{1}{3} \langle V^2 \rangle = \frac{1}{n} \int \frac{1}{3} V^2 f(\mathbf{v}, \mathbf{x}, t) d\mathbf{v}$ is the average fluctuating kinetic energy, expressed as the granular temperature.

The above conservation equations are supplemented by the constitutive relations for the stress, energy flux, and energy dissipation rate, which are expressed as functions of these fields,

$$\sigma_{ij} = m \int V_i V_j f(\mathbf{v}, \mathbf{x}, t) d\mathbf{v}, \quad (6)$$

$$\mathbf{q} = \frac{m}{2} \int \mathbf{V} V^2 f(\mathbf{v}, \mathbf{x}, t) d\mathbf{v}, \quad (7)$$

$$\Gamma = -\frac{m}{2} \int |\mathbf{v}|^2 J[f, f] d\mathbf{v}. \quad (8)$$

To solve this system of equations, first an approximate form of the function $f(\mathbf{v}, \mathbf{x}, t)$ is defined. Then the adoption of paired distribution function $f_2(\mathbf{v}_1, \mathbf{x}_1, t_1; \mathbf{v}_2, \mathbf{x}_2, t_2)$ is used to predict the collisional term, $J[f, f]$. The time evolution equation of the particle distribution function is then solved approximately for $f(\mathbf{v}, \mathbf{x}, t)$. Finally, the transport coefficients are calculated. In our calculations we adopt the solution procedures from the work of Garzó and Dufty^{30,31} which are formulated for smooth,

frictionless moderately inelastic particles in the dilute regime. In the absence of external forces, the constitutive relations of the model are given in Table I.

III. THE TC MODEL AND THE MODIFIED KINETIC THEORY

The standard approaches for the kinetic theory are derived by assuming that the kinetic energy of particles is only dissipated through binary, instantaneous collisions between particles. These approaches accurately capture the granular flow behavior in dilute flows but fail to do so for dense flows, where multi-particle collisions and finite-duration contacts are of significance. Because the kinetic theory does not account for the duration of contact in a dense regime, with the increase of collision frequency a particle can experience multiple collisions within a very short time. Since each collision incurs dissipation based on the kinetic theory, a significant overestimate of energy dissipation results. The event-based hard sphere (HS) model also suffers the same problem. In contrast, the soft-sphere DEM model requires a duration of contact for each collision, which makes it more realistic. In order to extend the kinetic theory to the dense flow regime, we consider the particle collision as a finite time process. Hence, we may apply the corresponding modifications to the kinetic theory to account for the more complex particle interactions.

Several researchers used the HS or IHS model to study particulate flows. In the IHS model, the particles are assumed to be perfectly rigid and to follow an undisturbed motion until

a collision occurs. Due to the rigidity of the interaction, the collisions occur instantaneously. In such cases an event-driven simulation method may be used. There are a few shortcomings with this method, namely, the inelastic collapse of particles, the neglect of multi-particle interactions, and the absence of the static limit. It was pointed out that all three problems have essentially one origin: the potential used between the centers of mass of the two colliding particles is artificially stiff.¹ To address these issues, Luding and Goldshtein²⁶ extended the IHS model by defining a duration of contact t_c , such that the dissipation of energy is allowed only if the time between inter-particle contacts is larger than t_c . The physical explanation for this is that there is a fraction of the total energy (e.g., the elastic potential energy) that is not dissipated for such a collision. When a system is very dense, the assumption of instant and binary collisions adopted in the classical kinetic theory is no longer valid. In this case, both the kinetic theory and the IHS cannot capture the enduring contact process and will over-predict the collision rate due to the unphysical stiffness, thus overestimating the energy dissipation rate. The dimensionless time ratio $\tau_c = t_c/t_E$ measures the existence of enduring and multi-body contact. Here, t_E is the inter-collision time as predicted by kinetic theory. In order to capture the elastic deformation process within a finite contact time, the implementation of the TC model in the IHS is simply to reset restitution coefficient e to 1 if a particle has a previous collision within a given t_c . This non-dissipative fraction is absent in all the idealized models such as hard-sphere, IHS, and the classical kinetic theory. Naturally, it leads to the over-prediction of the energy dissipation rate. As a result, a correction function, K , is multiplied to the dissipation term to account for the overestimate caused by multi-body collisions at high solid fractions, while the structure of the resulting theory remains the same. The correction function K is a function of the granular temperature T and the dimensionless time ratio $\tau_c = t_c/t_E$. Thus K is also the ratio of the kinetic energy to the total energy of kinetic energy and elastic potential energy. The contact duration t_c should be related to the particle properties. The average time between collisions t_E is obtained from the kinetic theory as follows:

$$t_E^{-1} = \frac{12}{d} \phi g_0 \sqrt{\frac{T}{\pi}}, \quad (9)$$

where d is the particle diameter, g_0 is the radial distribution function that is given in the Appendix, and ϕ is the solid volume fraction.³²⁻³⁴ To verify Eq. (9), we compared it with another expression proposed by Kumaran¹⁷ which is based on the DEM simulation results, as shown in Fig. 1. It is observed in the figure that the two equations produce very similar results up to $\phi = 0.62$, where their difference is 7%.

The correction function K may be derived from the probability of elastic collisions in a granular flow system.¹ We let the function $p(t_c)$ be the probability of a single particle that has no collision in the previous time interval t_c and its collision frequency is given as t_E^{-1} , so the probability of this particle to have no collision in the next dt interval is

$$p(t_c + dt) = p(t_c) (1 - t_E^{-1} dt). \quad (10)$$

A first order Taylor expansion of above equation yields

$$p(t_c) = \exp(-\tau_c). \quad (11)$$

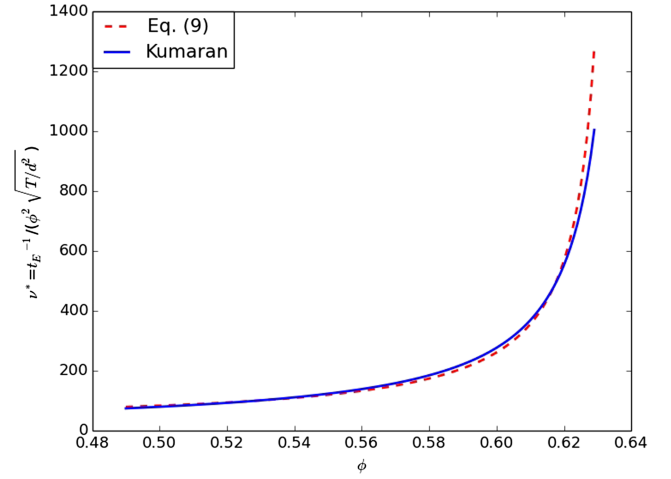


FIG. 1. The scaled collision frequency ν^* as a function of volume fraction ϕ . Comparison between Eq. (9) and the expression derived by Kumaran¹⁷ (Eq. 3.24 in his paper) based on the DEM simulation data, $\nu^* = \frac{11.039}{(0.64-\phi)}$.

The probability function $p(t_c)$ can be used to measure the fraction of “inelastic” particles in the system. Therefore, the total fraction of inelastic collisions in the system will be

$$K = p(t_c)^2 = \exp\left(-24 \frac{t_c}{d} \phi g_0 \sqrt{\frac{T}{\pi}}\right). \quad (12)$$

By fitting the kinetic theory results with the IHS results for the Homogeneous Cooling State (HCS) case, Luding and Goldshtein²⁶ obtained an empirical correlation for the function K ,

$$K = \exp(\psi(x)), \quad (13)$$

$$\psi(x) = -1.268x + 0.01682x^2 - 0.000578x^3 + O(x^4), \quad (14)$$

$$x = \sqrt{\pi\tau_c}. \quad (15)$$

Figure 2 shows the comparison between the derived function K from the kinetic theory in Eq. (12) and the empirical expression Eq. (13) from the HCS hard sphere simulation in Ref. 1. In general the two expressions match very well. A slight

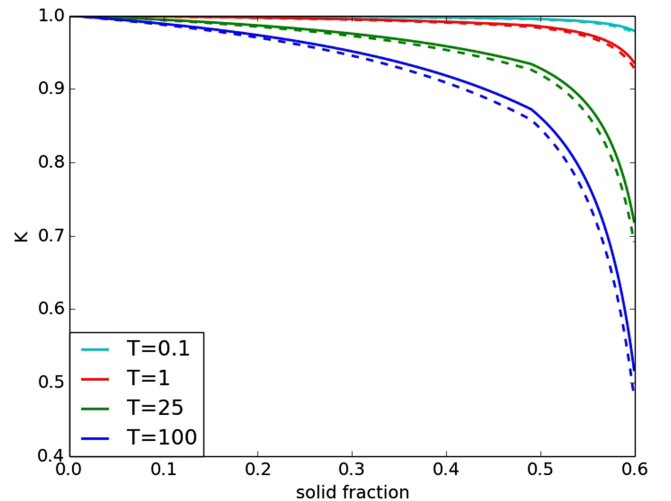


FIG. 2. K from Eq. (12) (solid lines) and the fitting expression of Eq. (13) (dashed lines) at different T .

difference is observed when the solid volume fraction or granular temperature is large. The difference is probably caused by the radial distribution function. For both equations, K is small at high granular temperature T and large solid fraction, ϕ , which is reasonable since the increase of granular temperature or the increase of solid volume fraction can increase the mean velocity of particles or shorten the mean free path between collisions and reduce the collision interval, making multi-body contacts prevail. From Eq. (12) we can see that if the solid volume fraction ϕ and the granular temperature T are very small, the scaled collision ratio τ_c will be close to zero and K will be close to one, reducing to the classical kinetic theory. In the dense region where the solid volume fraction ϕ is large, the values of radial distribution function g_0 are high, and K is much less than one, implying a significantly reduced dissipation rate. Similarly, increasing granular temperature T can also reduce K , but not as significantly as changing ϕ . Even at a low solid friction, high granular temperature in a system may also cause the failure of the kinetic theory.

As shown in Eq. (12), the correction function K strongly depends on the cutoff time t_c . In the original study for the HCS case, t_c is an adjustable parameter and it is chosen to match the kinetic theory results with the model results.¹

The inelastic collapse occurs in the IHS model but not in the DEM model because the DEM permits a duration of contact, t_{DEM} , during a collision. On the other hand, the value of t_c used in the MKT model is also a measure of the contact duration, so it has to be related to t_{DEM} . For a linear spring-dash collision model, we have

$$t_{DEM} = \pi \left(\frac{2k_n}{m} - \frac{\gamma_n^2}{4} \right)^{-1/2}, \quad (16)$$

where k_n is the normal spring constant and γ_n is the damping coefficient.³⁵ If we make $t_c = t_{DEM}$ and the particles have a larger spring constant k_n , it is apparent that the contact duration t_c will become small and K will be close to one. Therefore, the MKT resembles the classical kinetic theory at high stiffness. In Sec. IV we evaluate the MKT model with the use of $t_c = t_{DEM}$ and compare its results with those obtained by the kinetic theory model and the DEM model.

IV. RESULTS AND COMPARISONS WITH DATA

Due to the macroscopic size of the particles, external fields such as gravity would have a much stronger effect on granular flows. It is difficult to experimentally investigate the flow behavior of granular materials under shear in diluted to moderately dense regions. Instead, the Discrete Element Method (DEM) with a soft-sphere collision scheme is considered to be a more realistic model in modeling granular flows. The method uses a Lagrangian scheme to track each individual particle. The particles interact via a linear spring-dashpot (LSD) model, which gives the normal and tangential forces on a particle i caused by its contact with a particle j as follows:

$$F_{ij}^n = k_n \delta_{ij} - \gamma_n m_{eff} v_{ij}^n, \quad (17)$$

$$F_{ij}^t = -k_t u_{ij}^t - \gamma_t m_{eff} v_{ij}^t, \quad (18)$$

where δ_{ij} is the overlap distance and k_n and k_t are the spring coefficients in the normal and tangential directions. v_{ij}^n and v_{ij}^t are relative velocities in normal and tangential directions. The parameter $m_{eff} = m_i m_j / (m_i + m_j)$ is the effective mass of the two particle masses m_i and m_j . It has been reported that the contact dynamics of the particles are not very sensitive to the ratio k_t/k_n .^{35,36} In this study we chose the values $k_t/k_n = 2/7$ and $\gamma_t = 0$. The latter implies that there is no rotational velocity damping term in our simulations. If all the forces acting on the particle i are known, the problem is reduced to the integration of Newton's equations of motion for the translational and rotational degrees of freedom,

$$m_i \frac{d^2}{dt^2} \mathbf{r}_i = \mathbf{F}_i, \quad (19)$$

$$I_i \frac{d}{dt} \boldsymbol{\omega}_i = \mathbf{T}_i. \quad (20)$$

The position vector and angular velocity of particle i are \mathbf{r}_i and $\boldsymbol{\omega}_i$, respectively. I_i is the spherical particles moment of inertia. \mathbf{F}_i and \mathbf{T}_i are the force and torque by collisions. The DEM simulation time step Δt compared with the particle collision time t_{DEM} must be small in order to resolve accurately the particle collision process. For the computations we chose $\Delta t < t_{DEM}/50$, a practice successfully followed by others.³⁵⁻³⁷ The MFIX package,³⁸ which is available from the National Energy Technology Laboratory (NETL), was used to perform both the DEM and the continuum modeling simulations. The particles in the system were randomly distributed at $t = 0$, and the initial velocity distribution function was a Maxwellian distribution.

A. Homogeneous shear flow

Granular shear flows are quite complex; the hydrodynamic flow fields can be unsteady and vary across the flow domain. For the DEM simulations, a uniform shear rate can be imposed via the Lees-Edwards boundary condition.³⁹ Even for homogeneous shear flow, depending on the mechanics of particle contact, two regimes are distinguished: the first one is called inertial regime where the stresses arise from nearly instantaneous, binary collisions. The second one is called elastic or quasi-static regime where sustained multi-particle contacts prevail and the stresses are observed to be independent of shear rate. Only the reduction of solid concentration can cause a transition from an elastic regime to an inertial regime. Campbell⁴⁰ found that the granular flow behavior and flow regimes could be determined using $\frac{k}{\rho d^3 \gamma^2}$ and ϕ , as shown in Fig. 3. The kinetic theory works in the inertial regime with very low solid fractions because all particle interactions are binary and the transport rate is governed by the time between collisions and, thus, by the granular temperature. However the theory fails as the solid fraction increases and the flow gets close to the inertial no-collisional regime. In the elastic regime where more than two particles are in simultaneous contact, transport can occur between the particles through elastic waves traveling across the contact points—a rate which is governed by the elastic properties and not by the granular temperature.⁴⁰

Chialvo and Sundaresan⁹ conducted the DEM simulations of simple shear flows with a solid volume fraction ranging from

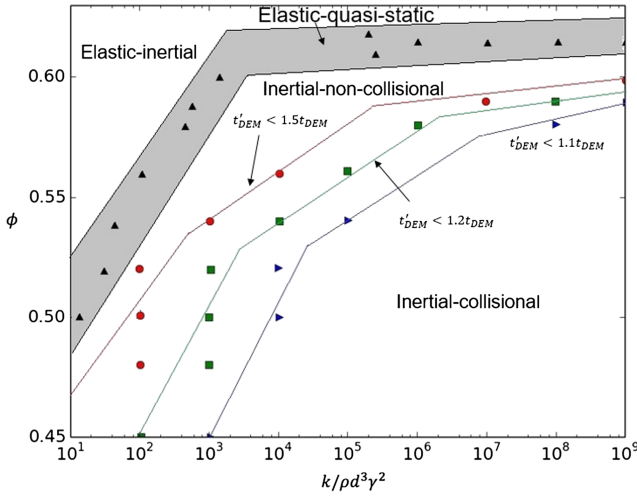


FIG. 3. Flow maps of the various flow regimes as presented by Campbell;⁴⁰ t'_{DEM} shows the averaged particle contact time in simulations and t_{DEM} is the theoretical binary contact time. Intermediate regime (i.e., elastic-inertial) only exists when $k/\rho d^3 \gamma^2$ is in certain range.

0.1 to 0.636 and covering both dilute and dense regimes. The simulation setup was accomplished by placing 2000 particles on a simple cubic lattice in a periodic box under uniform shear. The coefficient of restitution e , a property of particles collisions, varies from 0.7 to 0.99. Figure 4 shows the comparison of results between the classical kinetic theory model and the DEM model. It is clear that the kinetic theory results match well with the DEM results at low solid fractions ($\phi \leq 0.4$) where the flows are in the dilute regime. However, as the solid fraction increases to 0.5 or above, the results of kinetic theory model start to deviate from the DEM results, especially when the coefficient of restitution is high. This is expected since the kinetic theory model is built on the particle binary collision assumption and it fails in dense regimes where multi-particle collisions become more frequent. Hence, for flows in the regime of high solid fractions, the kinetic theory has to be modified to relax the binary collision assumption.

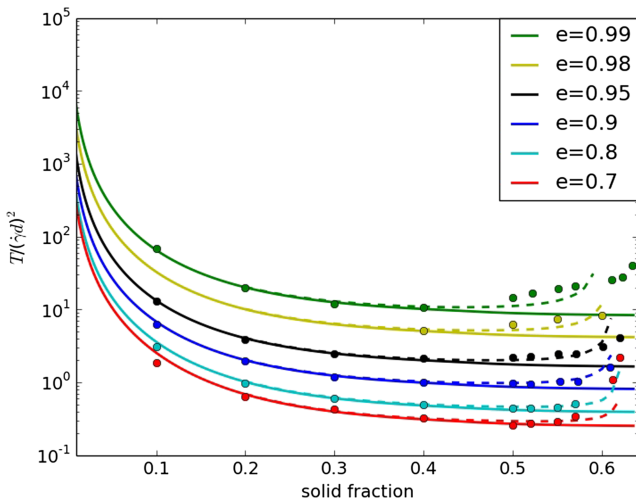


FIG. 4. The ratio of granular fluctuation energy to shear rate, $T/(\gamma d)^2$, versus the solids fraction ϕ in the uniform shear flow. The solid lines show the theoretical predictions by the KT. The dashed lines represent results by the current MKT and the discrete points represent the data from the DEM simulations of simple shear flow.⁹

We apply the MKT model with $t_c = t_{DEM}$ to study these cases. Figure 4 also compares the MKT results with the DEM results. It is seen that the MKT may capture well the trend of the increasing $T/(\gamma d)^2$ from dilute to moderately dense flow regimes up to solid fractions of 0.57. However, at very high solid fractions the system moves away from the inertial regime to the elastic regime, where many particles act together as force chains. In this case, the granular flow behaviors are no longer characterized by the particle collisions, and external forces are distributed through filament-like clusters of particles. The MKT predictions no longer agree with the DEM results.

The principal aim of the MKT model is to account for the effect of the elastic potential energy in the system that does not dissipate. This fraction of the elastic potential energy can be close to or even larger than the kinetic energy in the elastic regime.⁴¹ In the moderate dense regime, the accuracy of the MKT may deteriorate but it can still be valid when the system only has a small fraction of the elastic potential energy. However, the MKT eventually will fail when the fraction of the elastic potential energy becomes very large. In our case, the fraction of elastic potential energy is larger than 45% at a solid fraction of 0.57 and the MKT can still get reasonable predictions compared to the DEM results. We can also show the amount of the elastic potential energy in the system using a measured average contact time t'_{DEM} in the DEM simulations. The ratio of this measured contact time t'_{DEM} and the theoretical binary contact time t_{DEM} should be used as a probe to determine the flow regime shown in Fig. 3.⁴⁰ The ratio should be one if no multi-particle collisions exist. From Fig. 3 we can see that this ratio increases from 1 to 1.5 while flow remains in the inertial regime. The high ratio of t'_{DEM}/t_{DEM} indicates a significant amount of multi-particle collisions or a large amount of elastic potential energy. A significant departure from the rapid flow behavior was observed when $t'_{DEM}/t_{DEM} = 2$ at a solid fraction of 0.57 in another study.⁴²

It must be pointed out that the non-dimensional parameter $\frac{k}{\rho d^3 \gamma^2}$ is considered to be proportional to the square of the ratio of the free-flight time between shear-rate-induced particle-particle contacts and the time it takes the contact forces to drive the particles apart.⁴⁰ In simple shear flows, a small shear rate yields the small granular temperature in the system. With all other parameters fixed, the non-dimensional parameter $\frac{k}{\rho d^3 \gamma^2}$ becomes large, and the inertial-non-collisional regime becomes narrow on the regime map as shown in Fig. 3. The kinetic theory (KT) could remain accurate at a small shear rate in a wide range of solid volume fraction ϕ . This could also be explained by the MKT, because the discrepancy between MKT and kinetic theory becomes smaller and the fraction of inelastic collisions K will be close to one. According to Eq. (12), this is due to the small granular temperature at the low shear rates. With a larger shear rate, the mean free-flight time tends to be smaller and becomes comparable to the particle collision interval as predicted by the kinetic theory. The inertial-collisional regime becomes narrow on the map, making KT fail even for moderate dense flows, and we found that MKT tends to underestimate the dissipation rate due to the increasing granular temperature by the large shear rate. In

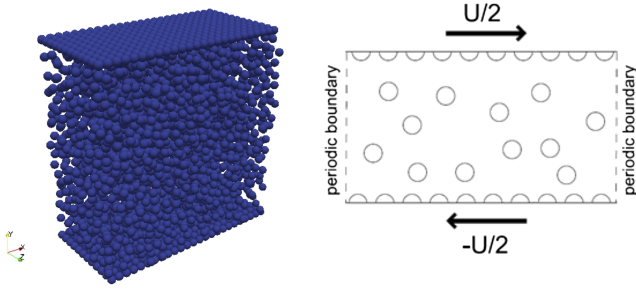


FIG. 5. Schematic diagram of particles being sheared between two plates.

this case, the cutoff time should be determined by the shear-induced time instead of the binary collision duration, so the use of $t_c = t_{DEM}$ is no longer appropriate. Nevertheless for flows in the inertial regime with high solid fractions, by using $t_c = t_{DEM}$ the MKT in general is able to improve the kinetic theory model and obtain results that agree well with the numerical DEM results.

B. Plane shear flow

We perform three-dimensional DEM simulations of the plane shear flows and compare its results with the MKT results. We make sure the solid volume fraction $\phi < 0.57$ across the domain and apply the MKT. By comparing with the original kinetic theory and another popular modification of kinetic theory or EKT, we evaluate the presented model under non-homogeneous shear flow conditions. Several granular flow simulation studies were performed with shear flow, but most of them assume the Lees-Edwards boundary condition,^{9,13,18,29} which is a special kind of periodic boundary condition that does not represent a real physical boundary. The hydrodynamic flow fields under the Lees-Edward boundary condition are always uniform. Other researchers simulated the sheared granular flows confined in frictional flat boundaries,^{43,44} but flows in their systems are not very dense. In addition, they introduced large slip velocities near the boundaries. The setup of boundaries in the present simulations is similar to the work by Saitoh and Hayakawa²⁵ where the spherical particles are attached to the top and bottom walls. The system is composed of identical, frictionless spheres, which are confined in a three-dimensional cube and sheared between two parallel planes, as shown in Figure 5. In this case, there is no interstitial fluid to provide hydrodynamic forces on the particles. The top plate has a velocity of $U/2$ directing to the right and the bottom plate has a velocity of $U/2$ to the left. The boundary conditions in the x and z directions are periodic. The simulation parameters are listed in Table II.

Figure 6 shows three two-dimensional section views of a plane through the center. As shown in Fig. 6(a), at $t=0$

TABLE II. Simulation parameters.

$D = 0.8$ cm
$\rho = 2700$ kg/m ³
$e = 0.9$
$L \times H \times W = 20$ cm \times 20 cm \times 10 cm
$U = 0.20$ m/s

the particles are uniformly distributed with random velocities. The particles collide freely without energy dissipation for enough time to ensure that they are randomly distributed and the velocities obey the Maxwellian distribution. Figures 6(b) and 6(c) show the time evolution of the particles' configuration for $\phi = 0.19$ and $\phi = 0.46$, respectively. It is observed that a high solid volume fraction particle cluster is formed in the center region, when the system reaches steady state, at $t = 60$ s. With a higher number of particles in the system, we observe larger clusters. The solid volume fraction in the center region approaches the maximum packing density, $\phi = 0.636$ during this transient, and finally is reduced to a lower value, which depends on the rate of shear. The simulations show that systems with small rates of shear have lower granular energy fluctuations at the core, which leads to the formation of denser clusters, i.e., higher solid volume fractions. Similar results were also observed in previous studies.^{25,45,46}

We modified the source code in the MFIX and implemented the contact duration theory in order to obtain a numerical solution that can be compared to the DEM results. The Johnson-Jackson boundary condition⁴⁷ was adopted for the solid phase to reproduce the rough wall in the DEM simulations. The force exerted on the boundary by the particles is the sum of collisional and frictional contributions. This yields the following momentum equation:

$$\frac{\mathbf{u}_{sl} \cdot (\boldsymbol{\sigma}_c + \boldsymbol{\sigma}_f) \cdot \mathbf{n}}{|\mathbf{u}_{sl}|} + \frac{\Psi_p \sqrt{3T} \pi \rho \phi |\mathbf{u}_{sl}|}{6\phi_c [1 - (\phi/\phi_c)^{1/3}]} + N_f \tan \delta = 0. \quad (21)$$

Here, \mathbf{u}_{sl} is the slip velocity between the particles and the wall; $\boldsymbol{\sigma}_c$ and $\boldsymbol{\sigma}_f$ are the collisional and frictional stress tensors, respectively; and \mathbf{n} is the unit normal vector to the wall. The first term on the left represents the internal solid collisional and frictional stress. The second term represents the rate of tangential momentum transfer to the wall by the particle-wall collisions. This is modeled as the product of the collision frequency for each particle, $(3T)^{1/2}/s$, where T is the granular temperature, the average tangential momentum transferred per collision, $\phi \pi \rho d^3 u_{sl}/6$, and the number of particles adjacent to unit area of the surface, $1/a_c$. The third term is the stress due to the sliding of the particles. The variable s denotes the average distance between the boundary and the surface of an adjacent particle: $s = d \left[\left(\frac{\phi_c}{\phi} \right)^{1/3} - 1 \right]$, $a_c = d^2 \left(\frac{\phi_c}{\phi} \right)^{2/3}$, $\phi_c = 0.636$, and Ψ_p is the specularity coefficient. In the cases considered here, the granular flow is not dense near the boundaries and the particle velocity distribution is mainly determined by inter-particle collisions rather than by the surface friction. For this reason, the internal frictional stress term is neglected and the last equation is written as

$$\frac{\mathbf{u}_{sl} \cdot \boldsymbol{\sigma}_c \cdot \mathbf{n}}{|\mathbf{u}_{sl}|} + \frac{\Psi_p \sqrt{3T} \pi \rho \phi |\mathbf{u}_{sl}|}{6\phi_c [1 - (\phi/\phi_c)^{1/3}]} = 0. \quad (22)$$

The Johnson-Jackson granular energy boundary condition is

$$-\mathbf{n} \cdot \mathbf{q}_{PT} = D - G, \quad (23)$$

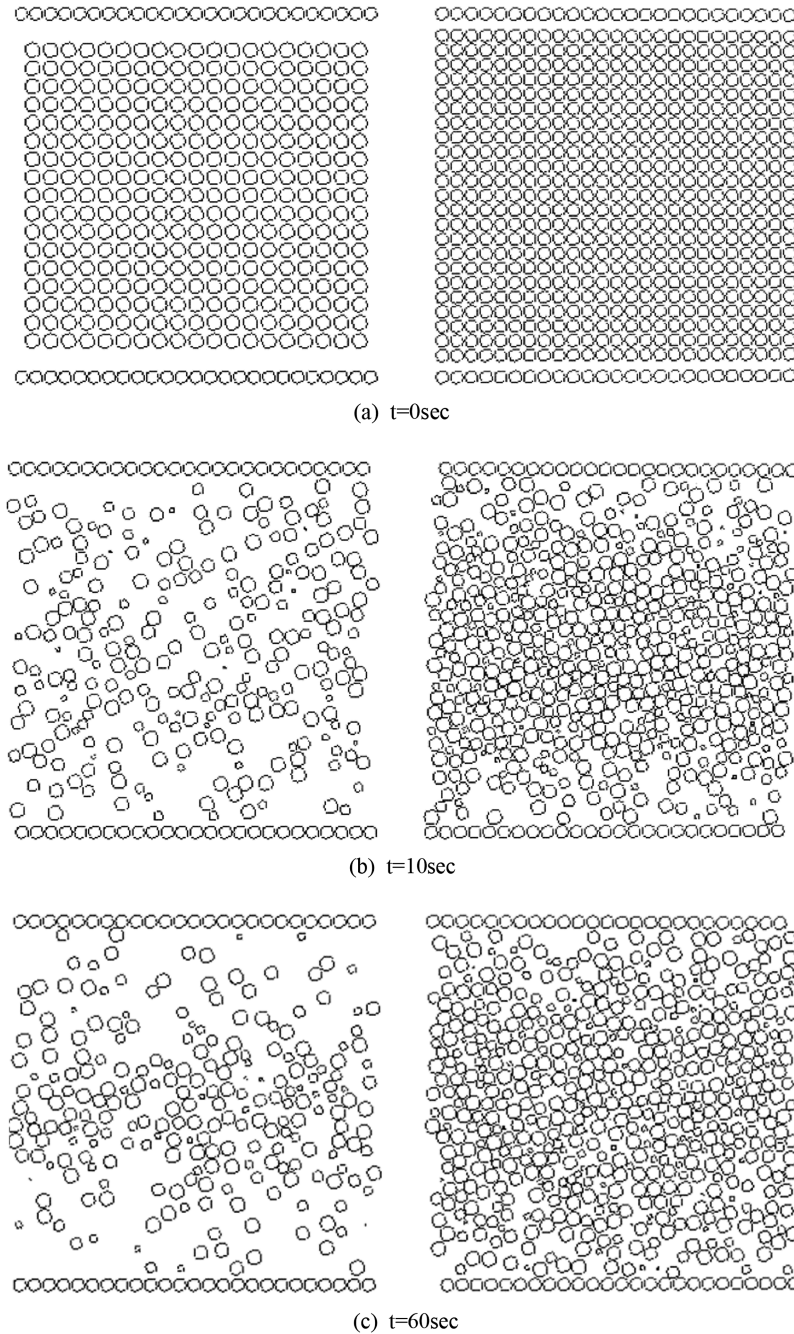


FIG. 6. Evolution of the configuration of particles (left: 3507 particles; right: 7500 particles).

where \mathbf{q} is the heat flux, D denotes the dissipation rate due to the particle-wall collisions, and G stands for the energy generation due to the particle-wall slip,

$$D = \left[\frac{1}{4} \pi \rho d^3 T (1 - e^2) \right] \left[\frac{\sqrt{3T}}{d \left[(\phi_c/\phi)^{1/3} - 1 \right]} \right] \left[\frac{1}{d^2 (\phi_c/\phi)^{2/3}} \right], \quad (24)$$

$$G = \frac{\Psi_p \sqrt{3T} \pi \rho \phi |\mathbf{u}_{sl}|}{6\phi_c \left[1 - (\phi/\phi_c)^{1/3} \right]}. \quad (25)$$

The above equations show that the particle-wall collisions are characterized by the transfer of momentum and the pseudo-thermal energy. The types of collisions are basically

determined by the specularity coefficient, Ψ_p , whose actual value depends on the large-scale roughness of the wall and varies between zero, for perfectly specular collisions, and one, for perfectly diffuse collisions. Previous studies have shown that this coefficient is small when only the collisions of spherical particles with plane frictional walls are considered because of the limited tangential momentum transfer between particles and plane walls.⁴⁸ In the cases considered here, we extend the Johnson-Jackson boundary condition by considering additional physical effects, namely, the wall roughness, and other boundary parameters, which are carefully chosen to match the slip velocity in the DEM simulations.

We have tested three cases with 3507 particles ($\phi = 0.19$), 5913 particles ($\phi = 0.35$), and 7500 particles ($\phi = 0.46$). The domain along the y -direction is divided in 20 slices to

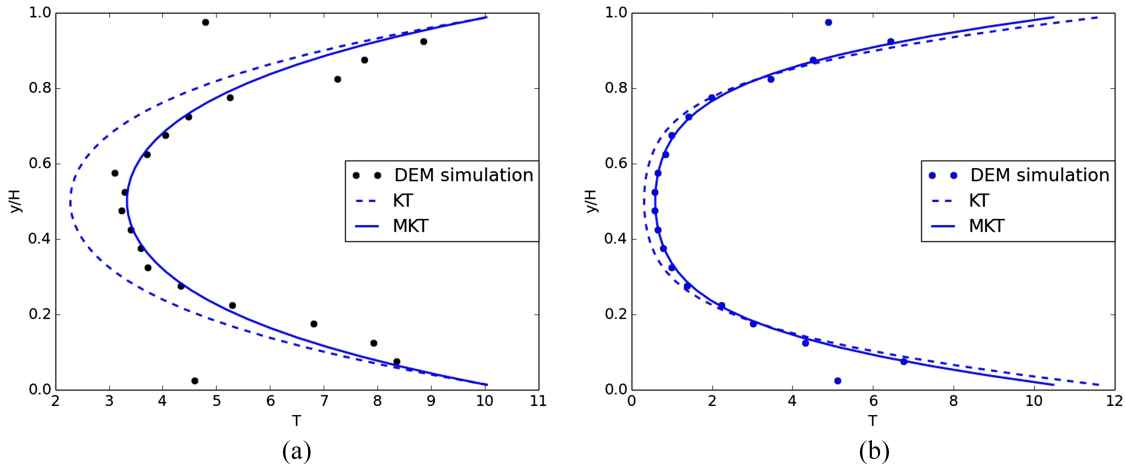


FIG. 7. Profile of granular temperature T along the y direction. DEM result (dots) and theoretical solution from the KT model (dashed line), theoretical solution from this model (line) at $e = 0.95$ (a) and $e = 0.9$ (b).

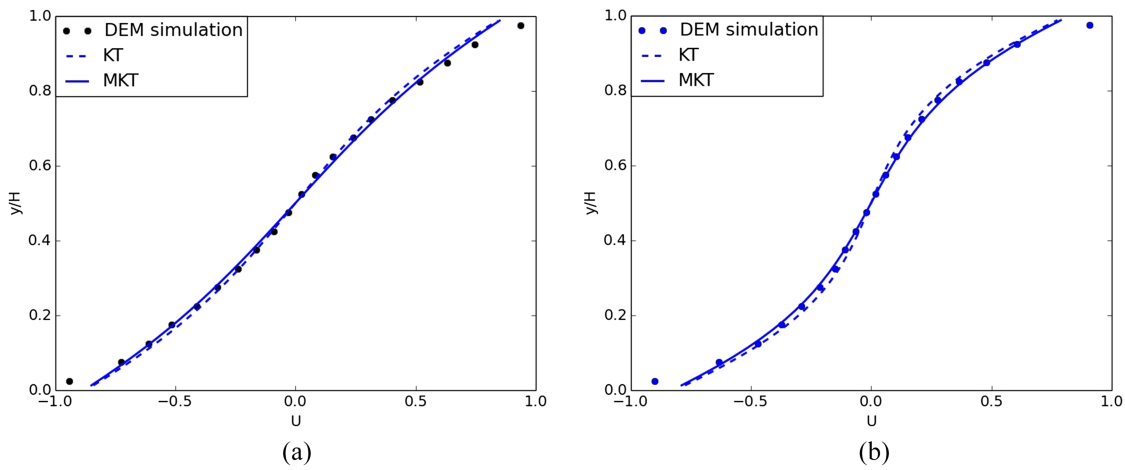


FIG. 8. Profile of average velocity $2u/U$ along the y . DEM result (dots) and theoretical solution from the KT model (dashed line), theoretical solution from this model (line) at $e = 0.95$ (a) and $e = 0.9$ (b).

perform the averaging. We used only the calculation for the dense case with 7500 particles. The number of particles in each slice is more than 280, and the resultant velocity/granular temperature profiles are very smooth along the y -direction.

The solid volume fraction profile is not very smooth because the slice length we used is rather narrow (about 1.2 times of particle diameter). Figures 7–9 compare the profiles of the variables u , T , and ϕ obtained from the DEM results with

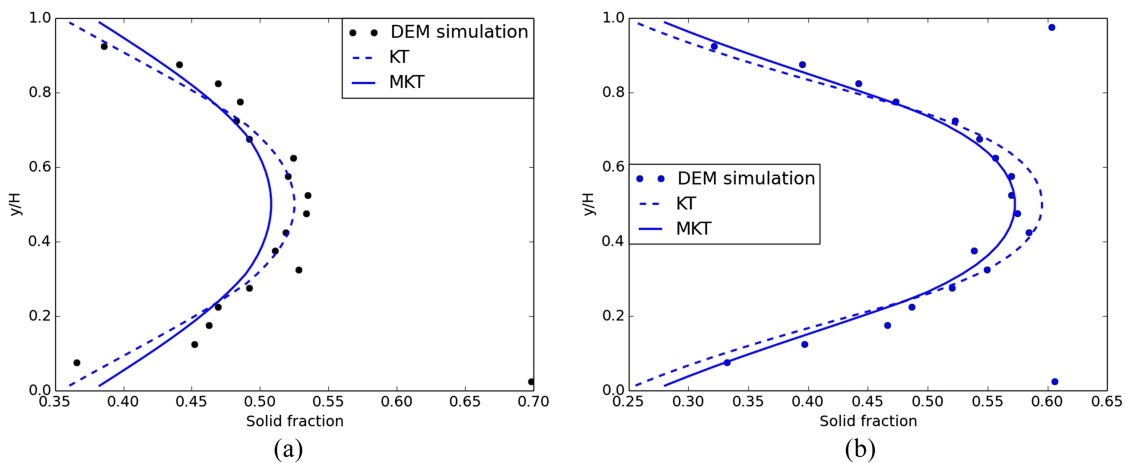


FIG. 9. Profile of solid volume fraction ϕ along the y direction. DEM result (dots) and theoretical solution from the KT model (dashed line), theoretical solution from this model (line) at $e = 0.95$ (a) and $e = 0.9$ (b).

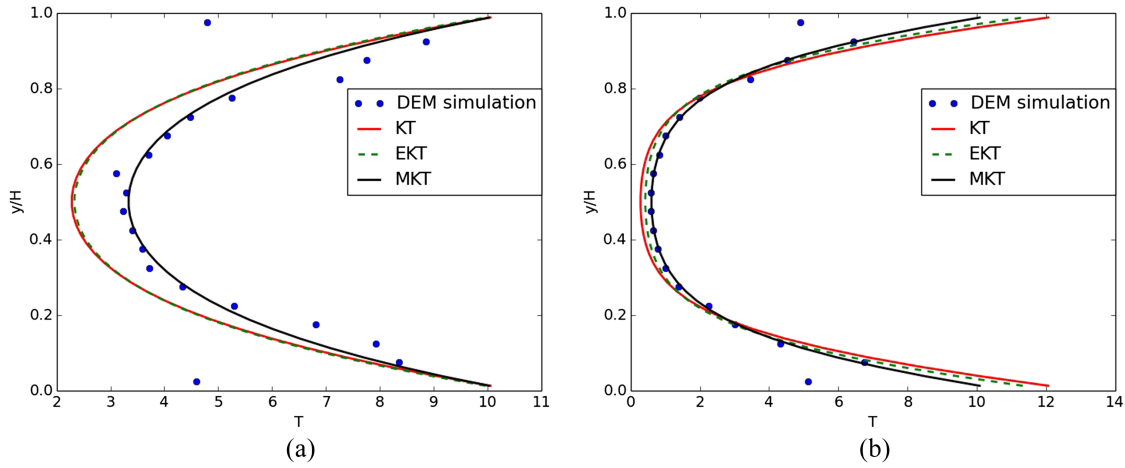


FIG. 10. Comparison of granular temperature results from the kinetic theory, the EKT, the MKT, and the DEM. (a) $e = 0.95$. (b) $e = 0.90$.

the theoretical solutions from both the classical kinetic theory and the MKT. We observe in Figure 8 that the velocity profile predictions of both theories agree well with the results of the DEM simulation. The velocity profiles are primarily determined by the boundary parameters (e.g., the specular coefficient) instead of the constitutive equations in the continuum approach. Due to the large number of boundary particles (fixed-velocity, no fluctuation energy), the averaged velocity and solid volume fraction data near the boundaries in DEM simulations are higher than normal, while the granular temperature is lower. These are shown as outliers in the velocity profiles.

It is also apparent that there is a cluster at the center, where the volume fraction of the solids is significantly higher than that near the wall, as shown in Fig. 9. The averaged granular temperature at the core for system with the higher inelastic coefficient $e = 0.95$ is more than twice the granular temperature value of in the system with $e = 0.9$. High granular temperature at the core means more particle collisions which helps prevent the clustering process. This is evident in Fig. 9 where the solid volume fraction at the core when $e = 0.95$ is significantly lower than that when $e = 0.9$ (0.53 vs 0.57). It is also observed that the kinetic theory predicts a lower core granular temperature than the DEM, as shown in Figure 7. This occurs because the core region in the center is denser, and multi-body collisions with longer lasting contacts prevail. As a result of this, the binary instant collision assumption is not valid and the classical theory overestimates the energy dissipation rate. The velocity and density profiles in Figs. 8(a) and 9(b), which were derived from the kinetic theory model, also have a noticeable discrepancy compared with the DEM results. From these results one may conclude that the MKT model, described in this paper, predicts the DEM results very well, even in the high solid volume fraction regions, where its predictions are more accurate than those of the kinetic theory model. Figure 10 also includes the results from the EKT model of the plane shear flow simulations. It can be seen that the EKT model does not produce better results for the nearly elastic particulate systems with restitution coefficient $e = 0.95$ and underestimates the granular temperature in the dense region when $e = 0.9$.

V. CONCLUSIONS

Most modifications of the kinetic theory aim to provide better agreement with the DEM simulation results. Compared with the DEM, the binary collision assumption behind the kinetic theory requires the spring constant of particles to be infinity. However, the spring constant is finite in the DEM simulations and in actual particulate collisions. This will make particle interaction a process that takes finite time to occur, and there will be elastic deformations during collisions. The large discrepancy observed between the kinetic theory prediction and DEM results at a high solid volume fraction comes from the particle softness that classical kinetic theory and most of its modifications did not consider. As a result of the finite spring constant, there exists significant amount of elastic deformation between particles in the dense region using DEM simulations. This means part of the kinetic energy that the kinetic theory predicts exists in the form of elastic potential energy in the DEM simulations and this form of energy cannot be dissipated during collisions. This also explains the overestimated dissipation rate predicted by the kinetic theory. To improve the current model, we modify the kinetic theory to consider elasticity of the particle. In this study we employ the MKT that is derived from the contact duration or cutoff time proposed in Ref. 1 and compare its results with the DEM results. The primary focus of our study is to evaluate the selection of the cutoff time t_c that can accurately predict the reduced dissipation rate as predicted by the DEM results so the applicability of KT can be extended to dense regime. Instead of treating the cutoff time as an adjustable number that best fits the IHS simulation results, we propose the use of a contact duration computed based on the DEM soft-sphere collision model, a parameter solely determined by particle properties, as the cutoff time and investigate its applicability. Two cases including the simple shear flow and the plane shear flow have been examined using the MKT model. For the simple shear flows, the MKT with $t_c = t_{DEM}$ is capable to predict results that match well with the DEM results when the flow is in the inertial regime, where particle collisions dominate. However, at a high solid fraction the flow falls into the elastic regime where particles form a “force chain” network, the cutoff time t_c depends on not

only t_{DEM} but also the shear rate so the MKT with $t_c = t_{DEM}$ fails. For the plane shear flow case where the shear rate and solid fraction are inhomogeneous, we find that the MKT with $t_c = t_{DEM}$ predicts very well the reduced dissipation rates and gives very good results, even in the dense particle regime with a solid fraction up to 0.57. We have shown that, overall, the MKT model is a significant improvement over the kinetic theory model. The accuracy of the present MKT model decreases in regions very close to the maximum packing density of the solids phase or at a very high shear rate. In these cases a cut-off time other than t_{DEM} has to be used or an improved MKT model has to be developed.

ACKNOWLEDGMENTS

This research work was supported by a grant from the U.S. Department of Energy (Award No. DE-FE0011453).

APPENDIX: RADIAL DISTRIBUTION FUNCTION

The radial distribution function g_0 we used was proposed by Torquato²³ and is based on the numerical results of elastic particles,

$$g_0 = \begin{cases} \frac{2 - \phi}{2(1 - \phi)^3}, & \text{if } \phi < 0.49, \\ \frac{(2 - 0.49) \cdot 0.636 - 0.49}{2(1 - 0.49)^3 \cdot 0.636 - \phi}, & \text{otherwise.} \end{cases} \quad (\text{A1})$$

- ¹S. Luding and S. McNamara, "How to handle the inelastic collapse of a dissipative hard-sphere gas with the TC model," *Granular Matter* **1**, 113 (1998).
- ²C. Lun, S. Savage, D. Jeffrey, and N. Chepurmy, "Kinetic theories for granular flow: Inelastic particles in Couette flow and slightly inelastic particles in a general flowfield," *J. Fluid Mech.* **140**, 223 (1984).
- ³J. Jenkins and M. Richman, "Kinetic theory for plane flows of a dense gas of identical, rough, inelastic, circular disks," *Phys. Fluids* **28**, 3485 (1985).
- ⁴K. Saitoh, *Kinetic Theory of Granular Gases* (University of Twente, 2012).
- ⁵S. Chialvo, *Constitutive Model Development for Flows of Granular Materials* (Princeton University, 2014).
- ⁶G. Bokkers, M. van Sint Annaland, and J. Kuipers, "Mixing and segregation in a bidisperse gas–solid fluidized bed: A numerical and experimental study," *Powder Technol.* **140**, 176 (2004).
- ⁷M. Van der Hoef, M. van Sint Annaland, N. Deen, and J. Kuipers, "Numerical simulation of dense gas-solid fluidized beds: A multiscale modeling strategy," *Annu. Rev. Fluid Mech.* **40**, 47 (2008).
- ⁸J. Chang, G. Wang, J. Gao, K. Zhang, H. Chen, and Y. Yang, "CFD modeling of particle–particle heat transfer in dense gas-solid fluidized beds of binary mixture," *Powder Technol.* **217**, 50 (2012).
- ⁹S. Chialvo and S. Sundaresan, "A modified kinetic theory for frictional granular flows in dense and dilute regimes," *Phys. Fluids* **25**, 070603 (2013).
- ¹⁰P. Jop, Y. Forterre, and O. Pouliquen, "A constitutive law for dense granular flows," *Nature* **441**, 727 (2006).
- ¹¹K. Kamrin, "Nonlinear elasto-plastic model for dense granular flow," *Int. J. Plast.* **26**, 167 (2010).
- ¹²K. Kamrin and G. Koval, "Nonlocal constitutive relation for steady granular flow," *Phys. Rev. Lett.* **108**, 178301 (2012).
- ¹³D. Berzi, "Extended kinetic theory applied to dense, granular, simple shear flows," *Acta Mech.* **225**, 2191 (2014).
- ¹⁴A. Srivastava and S. Sundaresan, "Analysis of a frictional–kinetic model for gas–particle flow," *Powder Technol.* **129**, 72 (2003).
- ¹⁵D. G. Schaeffer, "Instability in the evolution equations describing incompressible granular flow," *J. Differ. Equations* **66**, 19 (1987).

- ¹⁶A. S. Sangani, G. Mo, H.-K. Tsao, and D. L. Koch, "Simple shear flows of dense gas-solid suspensions at finite Stokes numbers," *J. Fluid Mech.* **313**, 309 (1996).
- ¹⁷V. Kumaran, "Dynamics of dense sheared granular flows. Part 1. Structure and diffusion," *J. Fluid Mech.* **632**, 109 (2009).
- ¹⁸N. Mitarai and H. Nakanishi, "Velocity correlations in dense granular shear flows: Effects on energy dissipation and normal stress," *Phys. Rev. E* **75**, 031305 (2007).
- ¹⁹J. T. Jenkins, "Dense shearing flows of inelastic disks," *Phys. Fluids* **18**, 103307 (2006).
- ²⁰J. T. Jenkins, "Dense inclined flows of inelastic spheres," *Granular Matter* **10**, 47 (2007).
- ²¹J. T. Jenkins and D. Berzi, "Dense inclined flows of inelastic spheres: Tests of an extension of kinetic theory," *Granular Matter* **12**, 151 (2010).
- ²²J. T. Jenkins and C. Zhang, "Kinetic theory for identical, frictional, nearly elastic spheres," *Phys. Fluids* **14**, 1228 (2002).
- ²³S. Torquato, "Nearest-neighbor statistics for packings of hard spheres and disks," *Phys. Rev. E* **51**, 3170 (1995).
- ²⁴R. A. Bagnold, *Experiments on a Gravity-Free Dispersion of Large Solid Spheres in a Newtonian Fluid Under Shear* (The Royal Society, 1954).
- ²⁵K. Saitoh and H. Hayakawa, "Rheology of a granular gas under a plane shear," *Phys. Rev. E* **75**, 021302 (2007).
- ²⁶S. Luding and A. Goldshtein, "Collisional cooling with multi-particle interactions," *Granular Matter* **5**, 159 (2003).
- ²⁷S. Chapman and T. G. Cowling, *The Mathematical Theory of Non-uniform Gases: An Account of the Kinetic Theory of Viscosity, Thermal Conduction and Diffusion in Gases* (Cambridge University Press, 1970).
- ²⁸J. Jenkins and S. Savage, "A theory for the rapid flow of identical, smooth, nearly elastic, spherical particles," *J. Fluid Mech.* **130**, 187 (1983).
- ²⁹D. Vescovi, "Granular shear flows: Constitutive modeling and numerical simulations," Ph.D. dissertation (Italy, 2014).
- ³⁰V. Garzó and J. Dufty, "Dense fluid transport for inelastic hard spheres," *Phys. Rev. E* **59**, 5895 (1999).
- ³¹S. Benyahia, M. Syamlal, and T. O'Brien, Summary of MFIX equations, available at <https://mfix.netl.doe.gov/documentation/MFIXEquations2012>, 2012.
- ³²S. Chapman and T. Cowling, *The Mathematical Theory of Nonuniform Gases* (Cambridge University, Cambridge, 1970).
- ³³T. Van Noije and M. Ernst, "Velocity distributions in homogeneous granular fluids: The free and the heated case," *Granular Matter* **1**, 57 (1998).
- ³⁴S. Luding, M. Huthmann, S. McNamara, and A. Zippelius, "Homogeneous cooling of rough, dissipative particles: Theory and simulations," *Phys. Rev. E* **58**, 3416 (1998).
- ³⁵L. E. Silbert, D. Ertas, G. S. Grest, T. C. Halsey, D. Levine, and S. J. Plimpton, "Granular flow down an inclined plane: Bagnold scaling and rheology," *Phys. Rev. E* **64**, 051302 (2001).
- ³⁶Y. Gu, A. Ozel, and S. Sundaresan, "A modified cohesion model for CFD–DEM simulations of fluidization," *Powder Technol.* **296**, 17 (2016).
- ³⁷Y. Gu, S. Chialvo, and S. Sundaresan, "Rheology of cohesive granular materials across multiple dense-flow regimes," *Phys. Rev. E* **90**, 032206 (2014).
- ³⁸M. Syamlal, W. Rogers, and T. J. O'Brien, "MFIX Documentation: Theory Guide", Technical Note DOE/METC-95/1013 and NTIS/DE95000031 (National Energy Technology Laboratory, Department of Energy, 1993).
- ³⁹A. Lees and S. Edwards, "The computer study of transport processes under extreme conditions," *J. Phys. C: Solid State Phys.* **5**, 1921 (1972).
- ⁴⁰C. S. Campbell, "Granular shear flows at the elastic limit," *J. Fluid Mech.* **465**, 261 (2002).
- ⁴¹Q. Sun, F. Jin, and G. G. Zhou, "Energy characteristics of simple shear granular flows," *Granular Matter* **15**, 119 (2013).
- ⁴²C. Campbell and Y. Zhang, "The interface between fluid-like and solid-like behavior in granular flows," *J. Fluid Mech.* **237**, 541 (1992).
- ⁴³M. Babic, "Unsteady Couette granular flows," *Phys. Fluids* **9**, 2486 (1997).
- ⁴⁴L. Popken and P. W. Cleary, "Comparison of kinetic theory and discrete element schemes for modelling granular Couette flows," *J. Comput. Phys.* **155**, 1 (1999).

- ⁴⁵S.-R. Kim, G. Maenhaut-Michel, M. Yamada, Y. Yamamoto, K. Matsui, T. Sofuni, T. Nohmi, and H. Ohmori, "Multiple pathways for SOS-induced mutagenesis in *Escherichia coli*: An overexpression of *dinB/dinP* results in strongly enhancing mutagenesis in the absence of any exogenous treatment to damage DNA," *Proc. Natl. Acad. Sci. U. S. A.* **94**, 13792 (1997).
- ⁴⁶D. Vescovi, D. Berzi, P. Richard, and N. Brodu, "Plane shear flows of frictionless spheres: Kinetic theory and 3D soft-sphere discrete element method simulations," *Phys. Fluids* **26**, 053305 (2014).
- ⁴⁷P. C. Johnson and R. Jackson, "Frictional–collisional constitutive relations for granular materials, with application to plane shearing," *J. Fluid Mech.* **176**, 67 (1987).
- ⁴⁸T. Li and S. Benyahia, "Revisiting Johnson and Jackson boundary conditions for granular flows," *AIChE J.* **58**, 2058 (2012).
- ⁴⁹S. Benyahia, M. Syamlal, and T. O'Brien, Summary of MFIx equations 2012-1, available at <https://mfix/.netl.doe.gov/documentation/MFIxEquations2012-1.pdf>, 2012.